Wind and Structures, Vol. 5, No. 6 (2002) 527-542
DOI: http://dx.doi.org/10.12989/was.2002.5.6.527

Dynamic crosswind fatigue of slender vertical structures

Maria Pia Repetto† and Giovanni Solari‡

DISEG, Department of Structural and Geotechnical Engineering, University of Genoa, Via Montallegro 1, 16145 Genoa, Italy

(Received October 10, 2001, Revised, July 22, 2002, Accepted August 29, 2002)

Abstract. Wind-excited vibrations of slender structures can induce fatigue damage and cause structural failure without exceeding ultimate limit state. Unfortunately, the growing importance of this problem is coupled with an evident lack of simple calculation criteria. This paper proposes a mathematical method for evaluating the crosswind fatigue of slender vertical structures, which represents the dual formulation of a parallel method that the authors recently developed with regard to alongwind vibrations. It takes into account the probability distribution of the mean wind velocity at the structural site. The aerodynamic crosswind actions on the stationary structure are caused by the vortex shedding and by the lateral turbulence, both schematised by spectral models. The structural response in the small displacement regime is expressed in closed form by considering only the contribution of the first vibration mode. The stress cycle counting is based on a probabilistic method for narrow-band processes and leads to analytical formulae of the stress cycles histogram, of the accumulated damage and of the fatigue life. The extension of this procedure to take into account aeroelastic vibrations due to lock-in is carried out by means of ESDU method. The examples point out the great importance of vortex shedding and especially of lock-in concerning fatigue.

Key words: buffeting; crosswind response; fatigue damage; fatigue life; lock-in; stress cycles histogram; vortex shedding.

1. Introduction

Wind-excited vibrations of structures can induce damage accumulation and cause structural failure without exceeding ultimate limit states. Some collapses due to wind loading have recently been attributed to fatigue (Robertson *et al*. 1999, Peil 2002).

Faced with the growing importance of this phenomenon and with the persistent lack of reliable calculation methods, the authors of this paper have recently developed a formulation to estimate the fatigue behaviour of slender vertical structures due to alongwind vibrations caused by longitudinal turbulence (Repetto and Solari 2001a).

Nevertheless, slender vertical structures exposed to wind may experience crosswind vibrations which are often more critical than alongwind vibrations and however characterised by different properties. In fact, the mean part of the response is usually negligible. The fluctuating part is due to the lateral turbulence and to the vortex wake. This constitutes a complex physical phenomenon that is often the main source of the vibration mechanism.

The vortex wake produces aerodynamic actions perpendicular to the wind direction, whose

† Scholarship Holder and PhD.
‡ Professor

frequency depends on the mean wind velocity and on the shape and the size of the structural section. The worst situation happens in correspondence of the critical wind velocities, which cause a resonant shedding with a natural frequency. In these conditions aeroelastic forces may exalt the motion up to realise an extremely dangerous synchronisation mechanism well known as lock-in. Since large vibrations often occur at moderate and frequent wind speeds, structures sensitive to this phenomenon may undergo a large number of stress cycles that cause fatigue damage.

In spite of numerous research works have been done in this field (Davenport 1966, Petrov 1998, Mikitarenko and Perelmuter 1998), not only crosswind fatigue can be dealt with as a fully open matter, but also the crosswind response of slender vertical structures (e.g., chimneys and towers) is a problem far to be solved definitely. In fact, several methods exist based on different physical and mathematical assumptions, which often lead to quite different results (Solari 1999).

According to the spectral model proposed by Vickery and Clark (1972), the actions caused by the vortex shedding on a stationary structure constitute a random stationary Gaussian process represented, in the frequency domain, by a power spectrum and a coherence function. When the Scruton number is large, the crosswind response may be calculated by the classical methods of random dynamics. When the Scruton number is small, the response becomes self-excited and sinusoidal. Using the method proposed by Vickery and Basu (1983) aeroelastic effects can be modelled by a non-linear aerodynamic damping.

Consistently with the above spectral model, ESDU (*Response of Structures* 1996) introduces a method where aeroelastic effects are taken into account by a mode-generalized fluctuating lift coefficient, as a non-linear function of the motion. It also assumes that, in the atmospheric wind, the amplitude of the motion may change over irregular periods from forced to self-excited and viceversa. Thus, a time factor is introduced, which represents the fraction of time during which the response is sinusoidal. It increases on decreasing the turbulence intensity and the Scruton number.

The vortex-resonance model proposed by Ruscheweyh (1994) mainly focuses on aeroelastic effects. Using a deterministic approach, it assumes that vortex shedding produces a harmonic force on the effective correlation length, expressed as a nonlinear function of the motion amplitude. This method has been introduced into the Eurocode 1 (1994) and is the basis of the only procedure currently in use for evaluating the vortex-induced fatigue. In such a context, the number of stress cycles during the structural life is evaluated taking in account the probability that the mean wind velocity occurs within a conventional velocity range centred in the critical velocity value.

This paper proposes a mathematical method for evaluating the crosswind fatigue of slender vertical structures, which represents the dual formulation of a parallel method (Repetto and Solari 2001a) that the authors recently developed with regard to alongwind vibrations. Likewise the companion alongwind procedure, this method takes into account the probability distribution of the mean wind velocity at the structural site. The aerodynamic crosswind actions on the stationary structure are caused by the vortex shedding and by the lateral turbulence, both schematised by spectral models. The structural response in the small displacement regime is expressed in closed form by considering only the contribution of the first vibration mode (Piccardo and Solari 2000). The stress cycle counting is based on a probabilistic method for narrow-band processes. The results provide analytical formulae of the histogram of the stress cycles, of the accumulated damage and of the fatigue life. The extension to large vibrations due to lock-in effects is carried out by means of ESDU method. Independently of its reliability or of its consensus with reference to the other methods previously cited, it seems to be the most appropriate to correct the above fatigue analysis in order to account for aeroelastic effects.

The proposed method is applied to three steel chimneys of different characteristics. The applications focus on the relative importance of the two components of the crosswind actions, i.e., the vortex shedding and the lateral turbulence, and furnish relevant elements for a deep comprehension of the physical phenomenon. The comparison with Monte Carlo simulations underlines the good agreement with numerical results.

2. Undisturbed wind

Let x, y, z be a Cartesian reference system with origin O on the ground and axis z directed upwards. Ignoring, for sake of simplicity, the dependence of the wind direction on the time t, the instantaneous wind velocity $\boldsymbol{U}$ at height z is expressed by the vectorial temporal law:

$$\boldsymbol{U}(z, t) = \overline{\boldsymbol{U}}(z, t)+\boldsymbol{u}(z, t) \tag{1}$$

in which $\overline{\boldsymbol{U}}$ and $\boldsymbol{u}$ are, respectively, the macro-meteorological and the micro-meteorological components of $\boldsymbol{U}$ (Van de Hoven 1957). It is admitted that $\overline{\boldsymbol{U}}$ varies so slowly in time to be approximated by a series of constant values on successive ΔT intervals (Fig. 1). On each ΔT interval, Eq. (1) becomes:

$$\boldsymbol{U}(z, t) = \overline{\boldsymbol{U}}(z)+\boldsymbol{u}(z, t) \tag{2}$$

where $\boldsymbol{u}(z, t)$ is the vectorial zero mean turbulent fluctuation of $\boldsymbol{U}$ around $\overline{\boldsymbol{U}}$.

Considering a flat homogeneous terrain and the internal boundary layer, $\overline{\boldsymbol{U}}$ and $\boldsymbol{u}$ result:

$$\overline{\boldsymbol{U}}(z)=\boldsymbol{i}\overline{U}(z) \tag{3}$$

$$\boldsymbol{u}(z, t) = \boldsymbol{i}u(z, t)+\boldsymbol{j}v(z, t)+\boldsymbol{k}w(z, t) \tag{4}$$

where $\boldsymbol{i}, \boldsymbol{j}, \boldsymbol{k}$ are the unit vectors in the directions x, y, z, $\overline{U}$ is the mean wind velocity aligned with x; u, v, w are the longitudinal (x), lateral (y) and vertical (z) turbulence components.

The mean wind velocity $\overline{U}(z)$ is expressed in terms of the height and the site properties, using the logarithmic profile as proposed in the Eurocode 1 (1994):

$$\overline{U}(z) \;=\; \overline{U}_{ref} k_T \ln\frac{z}{z_0} \tag{5}$$

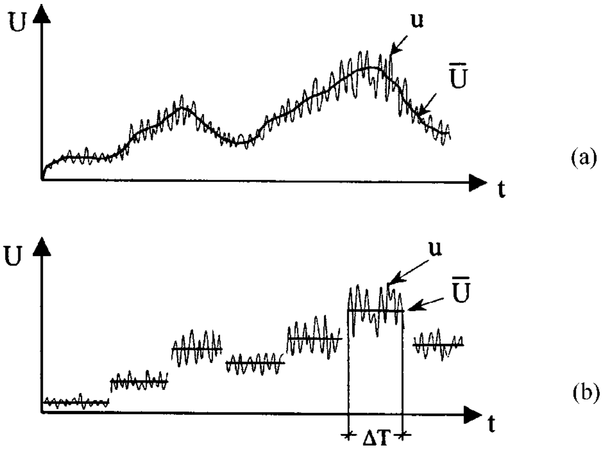

Fig. 1 Temporal representation of wind velocity: a) real; b) simplified

where k_T is the terrain factor and z_0 is the roughness length. $\overline{U}_{ref}$ is the reference velocity, i.e., the mean wind velocity at 10 m height, in open country; this is treated as a random variable whose distribution function is given by the hybrid Weibull model (Solari 1996):

$$F_{\overline{U}_{ref}}(\overline{U}_{ref}) = F_0 + (1-F_0)\left\{1-\exp\left[-\left(\frac{\overline{U}_{ref}}{c}\right)^k\right]\right\}, \quad \overline{U}_{ref} \geq 0 \tag{6}$$

in which F_0 is the probability that $\overline{U}_{ref}=0$; k e c are model parameters.

Turbulence components are schematized by random stationary Gaussian processes. A wide critical survey on turbulence models is provided, for instance, in Solari and Piccardo (2001).

3. Aerodynamic crosswind actions

The structure is schematised by a slender vertical beam, coaxial with z, of total height h, restrained at its base. Wind gives rise to complex aerodynamic phenomena which induce alongwind forces, crosswind forces and torsional moments (Piccardo and Solari 2000); at this stage of the analysis, aeroelastic effects are ignored. Focusing attention on only the crosswind response and treating xz as a symmetry plane, the mean wind force in y direction is null and its fluctuating component results:

$$f(z,t)=f_v(z,t)+f_\omega(z,t) \tag{7}$$

where f_v and f_ω are lateral turbulence and wake contributions, respectively.

Applying the quasi-steady theory and admitting that turbulence is small, the loading term associated with the lateral turbulence is given by:

$$f_v(z,t) = \frac{1}{2}\rho(c_d + c'_1)b\gamma_v(z)I_v(z)\overline{U}^2(z)v^*(z,t) \tag{8}$$

where ρ is the air density, c_d is the drag coefficient, c'_1 is the prime angular derivative of the lift coefficient, b is the reference size of the cross-section, $I_v(z)=\sigma_v/\overline{U}(z)$ is the lateral turbulence intensity, σ_v is the root mean square (rms) value of v, $v^*(z,t)=v(z,t)/\sigma_v$ is the reduced turbulence component, $\gamma_v(z)$ is a non-dimensional function of z, called v shape function, which makes this model suitable to be applied both to structures with variable aerodynamic properties and to non-prismatic structures.

The loading term associated with the wake excitation may be formally expressed by:

$$f_\omega(z,t) = \frac{1}{2}\rho\tilde{c}_{1\omega}b\gamma_\omega(z)\overline{U}^2(z)\omega_y^*(z,t) \tag{9}$$

where $\tilde{c}_{1\omega}$ is the rms lift wake coefficient, ω_y^* is the y reduced component of the wake excitation, treated as a random stationary Gaussian process (Vickery and Clark 1972), γ_ω is the ω shape function.

The cross-power spectra of v^* and ω^* have the general expression:

$$S^*_{\varepsilon\varepsilon}(z,z',n) = \sqrt{S^*_\varepsilon(z,n)S^*_\varepsilon(z',n)}\,\mathrm{Coh}_{\varepsilon\varepsilon}(z,z',n) \quad (\varepsilon=v,\ \omega) \tag{10}$$

where n is the frequency; $S^*_\varepsilon(z,n)$ is the power spectrum of the reduced excitation component ε^* at height z; $\mathrm{Coh}_{\varepsilon\varepsilon}(z,z',n)$ is the ε coherence function at heights z and z', assumed as real and given by the relationship:

$$\mathrm{Coh}_{\varepsilon\varepsilon}(z, z', n) = \exp\left\{-\kappa_\varepsilon(z, z', n)\frac{|z-z'|}{h}\right\} \tag{11}$$

where κ is a suitable non-dimensional quantity.

Appendix I provides the expressions of S_ε^* and κ_ε used in this paper.

Since f is a linear function of v^* and ω^* (Eq. 7), likewise v^* and ω^* also f is a random stationary Gaussian process. Furthermore, assuming v^* and ω^* as independent (Solari 1985), the cross-power spectrum of f is the sum of the cross-power spectra of f_v and f_ω (Eqs. 8 and 9).

4. Dynamic response and stress state

Let us consider the structure as linear elastic, with viscous damping.

The nil mean fluctuating crosswind force $f(z, t)$ (Eq. 7) produces a nil mean fluctuating crosswind displacement $y(z, t)$ that determines a nil mean fluctuating stress state. Let $s(z, t)$ denote the stress in a given point P of the cross-section at height z. Due to linearity, both y and s are random stationary Gaussian processes whose definition in general calls for numerical analysis (Solari 1986). The problem may be simplified assuming, as classically, that the response depends only on the first mode of vibration. In such a case, the power spectrum of the fluctuating stress is given by:

$$S_s(P, n) = [\bar{S}^x(P)]^2|H_{y1}(n)|^2[\chi_v^2 S_{veq}^*(n) + \chi_\omega^2 S_{\omega eq}^*(n)] \tag{12}$$

$\bar{S}^x(P)$ being the stress in P produced applying, in y direction, the alongwind mean force $\bar{F}(z)$:

$$\bar{F}(z) = \frac{1}{2}\rho c_d b \gamma_u(z)\bar{U}^2(z) \tag{13}$$

$H_{y1}(n)$ is the mechanical admittance function of the first mode of the structure:

$$H_{y1}(n) = \frac{1}{1-\left(\frac{n}{n_{y1}}\right)^2 + 2i\xi_{y1}\frac{n}{n_{y1}}} \tag{14}$$

where i is imaginary unit, n_{y1} and ξ_{y1} are the fundamental frequency and the damping coefficient of the first mode in y direction, respectively. χ_v and χ_ω are the non-dimensional quantities:

$$\chi_v = \frac{(c_d + c_1')I_v(h)K_v'}{c_d\bar{K}_{yu}} \tag{15}$$

$$\chi_v = \frac{\tilde{c}_{1\omega}K_\omega'}{c_d\bar{K}_{yu}} \tag{16}$$

where $\bar{K}_{yu}$, K_v' and K_ω' are non-dimensional coefficients expressed by:

$$\bar{K}_{yu} = \frac{1}{h\bar{U}^2(h)\phi_{y1}(h)}\int_0^h \bar{U}^2(z)\gamma_u(z)\phi_{y1}(z)dz \tag{17}$$

$$K'_v = \frac{1}{h\overline{U}^2(h)I_v(h)\phi_{y1}(h)}\int_0^h \overline{U}^2(z)\gamma_v(z)I_v(z)\phi_{y1}(z)dz \tag{18}$$

$$K'_\omega = \frac{1}{h\overline{U}^2(h)\phi_{y1}(h)}\int_0^h \overline{U}^2(z)\gamma_\omega(z)\phi_{y1}(z)dz \tag{19}$$

$\phi_{y1} \simeq (z/h)^{\zeta_{y1}}$ is the first modal shape in y direction, ζ_{y1} being a modal shape factor. $S^*_{veq}(n)$ and $S^*_{\omega eq}(n)$ are the reduced Generalized Equivalent Spectra (Piccardo and Solari 1998) of the lateral turbulence and of the wake excitation, respectively :

$$S^*_{veq}(n) = S^*_v(z_{yv}, n)C\left\{k_{yv}\frac{nC_{zv}h}{\overline{U}(z_{yv})}\right\} \tag{20}$$

$$S^*_{\omega eq}(n) = S^*_\omega(z_{y\omega}, n)C\left\{k_{y\omega}\frac{h}{Lb}\right\} \tag{21}$$

where :

$$C\{\chi\} = \frac{1}{\chi} - \frac{1}{2\chi^2}(1 - e^{-2\chi}) \text{ per } \chi > 0; \quad C\{0\} = 1 \tag{22}$$

$z_{yv} = 0.6\,h$ and $z_{y\omega} = 0.8\,h$ are the reference co-ordinates; $k_{yv} = k_{y\omega} \simeq 0.5/(\zeta_{y1} + 1)^{0.55}$ are the equivalent correlation factors (Piccardo and Solari 2001).

The knowledge of the power spectrum in Eq. (12) enables to obtain the main parameters of the stress process; in particular, desiring to count fatigue cycles, the rms value and the expected frequency should be determined. Taking Eq. (7) into consideration, the variance of the stress process can be expressed by :

$$\sigma_s^2(P) = \sigma_{sv}^2(P) + \sigma_{s\omega}^2(P) \tag{23}$$

in which $\sigma_{sv}^2(z)$ and $\sigma_{s\omega}^2(z)$ are the contributions to the total variance of the stress process due to the lateral turbulence and to the wake excitation, respectively. They are given by :

$$\sigma_{s\varepsilon}^2(P) = [\overline{S}^x(P)\,\chi_\varepsilon]^2(Q_\varepsilon + D_\varepsilon) \tag{24}$$

where Q_ε and D_ε are non-dimensional quantities proportional, respectively, to the quasi-static part and to the resonant part of the structural response to the ε excitation component :

$$Q_\varepsilon = \int_0^{n_{y1}} S^*_{\varepsilon eq}(n)dn \; ; \; D_\varepsilon = \frac{\pi n_{y1}}{4\xi_{y1}}S^*_{\varepsilon eq}(n_{y1}) \tag{25}$$

Using these quantities, the expected frequency of the stress process is given by :

$$v_s = \left[\frac{\chi_v^2 n_{y1}^2 D_v + \chi_\omega^2 n_{y1}^2 D_\omega}{\chi_v^2(Q_v + D_v) + \chi_\omega^2(Q_\omega + D_\omega)}\right]^{1/2} \tag{26}$$

Appendix II provides closed formulae of Q_ε and D_ε ($\varepsilon = \nu, \omega$) based on the spectral models defined in Appendix I (Piccardo and Solari 2000).

5. Stress cycles histogram and fatigue verification

The histogram of the stress cycles, the total accumulated damage and the fatigue life due to crosswind vibrations can be determined by the same procedure already used for analysing the alongwind fatigue in Repetto and Solari (2001a).

Let $\delta\overline{U}$ be a suitably small velocity range. $\overline{U}_{ref}$ values are subdivided into a full set of non-overlapping intervals $\Delta\overline{U}_i = (i-1, i)\,\delta\overline{U}\,(i = 1, 2, \ldots)$, centred on $\overline{U}_{ref,i} = (2i-1)\,\delta\overline{U}/2$. The sub-set of wind actions and the corresponding stress states associated with $\overline{U}_{ref}$ values belonging to $\Delta\overline{U}_i$ are referred to as the i-th loading condition. Its occurrence probability is given by:

$$P_i = (1-F_0)\left\{\exp\left[-\left(\frac{(i-1)\delta\overline{U}}{c}\right)\right]^k - \exp\left[-\left(\frac{i\delta\overline{U}}{c}\right)\right]^k\right\} \quad (i = 1, 2, \ldots) \tag{27}$$

The stress fluctuation s_i associated with the i-th loading condition is a nil mean Gaussian stationary random process, whose standard deviation σ_{si} and expected frequency ν_{si} are given by Eqs. (23) and (26), respectively, having put $D_\varepsilon = D_{\varepsilon i}$, where $D_{\varepsilon i}$ is the value of D_ε calculated in correspondence with $\overline{U}_{ref} = \overline{U}_{ref,i}$. It is admitted, as it is typical of flexible and lightly damped structures, that s_i is a narrow band process. Thus, at every up-crossing of a given S threshold, a cycle of amplitude $\Delta s \geq 2S$ corresponds.

Let us consider a series of stress thresholds $S_j = j\delta s$ ($j = 0, 1, 2, \ldots$), δs being a suitably small stress interval. Let $\Delta s_j = S_{j-1} + S_j = (2j-1)\,\delta s$ represent the average amplitude of the stress cycles in the range $(2S_{j-1}, 2S_j]$. The mean number of cycles of amplitude Δs_j per unit time, due to the i-th loading condition is given by:

$$n_{ij} = P_i \nu_{si}\left\{\exp\left[-\frac{(j-1)^2\,\delta s^2}{2\sigma_{si}^2}\right] - \exp\left[-\frac{j^2\,\delta s^2}{2\sigma_{si}^2}\right]\right\} \tag{28}$$

which provides the 3D stress cycles histogram.

Applying the Palmgreen-Miner linear accumulation law, the mean total damage D per unit time is the sum of the contributions to damage of all the blocks of the 3D stress cycles histogram:

$$D = \sum_i \sum_j d_{ij} \tag{29}$$

where d_{ij} is the fraction of the mean damage per unit time caused to the structure by the i, j-th block:

$$d_{ij} = \frac{n_{ij}}{N_j} \tag{30}$$

in which n_{ij} is given by Eq. (28) and N_j is the mean number of stress cycles with amplitude Δs_j which causes the structural collapse. Applying the experimental results obtained by Wohler, this can be expressed as a broken line in which the l-th segment is given by:

$$N_j = \frac{a_l}{\Delta s_j^{m_l}} \quad (\Delta s^{(l-1)} \leq \Delta s_j \leq \Delta s^{(l)}) \tag{31}$$

where a_l and m_l are parameters depending on the properties of the element studied.

Substituting Eqs. (28) and (30) into Eq. (29) provides the mean total damage per unit time. The fatigue life of the structure is the time period in which the mean total damage reaches the unit :

$$T_F = \left[\sum_i \sum_j \nu_{si} P_i \frac{1}{N_j}\left(\exp\left[-\frac{(j-1)^2 \delta s^2}{2\sigma_{si}^2}\right] - \exp\left[-\frac{(j\,\delta s)^2}{2\sigma_{si}^2}\right]\right)\right]^{-1} \tag{32}$$

6. Lock-in effects

Let us define the critical wind velocity $\overline{U}_{cr}$ as the mean wind velocity in correspondence of which the vortex shedding frequency $n_{y\omega}$ equals the fundamental frequency of the structure n_{y1} at the reference height $z = z_{y\omega}$. It is defined by :

$$\overline{U}_{cr} = \frac{n_{y1} b_m}{S} \tag{33}$$

in which b_m is the mean size of the upper third of the structure, S is the Strouhal number. When this condition occurs, lock-in effects may arise, whose importance depends on the Scruton number :

$$Sc = \frac{4\pi m_{y1} \xi_{y1}}{\rho b_m^2} \tag{34}$$

where m_{y1} is the first equivalent mass in y direction (Ruscheweyh 1994), very close to the average mass of the upper third of the structure.

When the Scruton number is sufficiently large, the response of the structure is forced by the vortex shedding and random in nature. The rms value and the expected frequency of the crosswind response can be evaluated using classical linear random dynamics and the fatigue life is appropriately furnished by the method described in the previous section.

On decreasing the Scruton number, the structural motion significantly affects the vortex shedding. The fluctuating forces at various sections along the structure tend to become in phase with the motion and thus more correlated with each other. The resulting response, defined as self-excited or locked-in, becomes nonlinear, deterministic and progressively assumes the shape of a constant amplitude sinusoid at frequency n_{y1}. Several methods have been proposed in literature to take these phenomena into account (Vickery and Basu 1983, Ruscheweyh 1994, *Response of Structures* 1996). Independently of the reliability or of the consensus related to different methods, which is still a matter of wide debate, the method proposed by ESDU seems to be the most appropriate to correct the above procedure for evaluating the role of lock-in effects on the fatigue life of the structure. Note, however, that ESDU method works with circular cross-sections. It can be used also for polygonal sections with eight or more sides, by equating the polygonal shape to an equivalent circular cylinder with added roughness.

In a neighbourhood of the critical wind velocity the amplitude of the motion can change over irregular periods from forced to self-excited and vice-versa. ESDU defines a time factor $f_t = f_t(Sc, \overline{U}, I_u)$, where I_u is the longitudinal turbulence intensity, which represents the fraction of time during which the response is sinusoidal; $(1\text{-}f_t)$ is the fraction of time during which the response is random.

On increasing Sc, or I_u, or for $\overline{U}$ far from $\overline{U}_{cr}$, f_t tends to zero. On decreasing Sc and I_u, and for $\overline{U}$ tending to $\overline{U}_{cr}$, f_t tends to be unit.

Based on this approach, the cycle histogram and the fatigue life derived assuming the structure as stationary (Eqs. 28 and 32) must be reviewed to take into account the fraction of time during which the self-excited response occurs. It results:

$$n_{ij} = (1-f_{ti})P_i\nu_{si}\left\{\exp\left[-\frac{(j-1)^2\delta s^2}{2\sigma_{si}^2}\right] - \exp\left[-\frac{j^2\delta s^2}{2\sigma_{si}^2}\right]\right\} + f_{ti}P_i n_{y1}k_{ij} \tag{35}$$

$$T_F = \left[\sum_i\sum_j(1-f_{ti})P_i\nu_{si}\frac{1}{N_j}\left\{\exp\left[-\frac{(j-1)^2\delta s^2}{2\sigma_{si}^2}\right] - \exp\left[-\frac{j^2\delta s^2}{2\sigma_{si}^2}\right]\right\} + f_{ti}n_{y1}P_i k_{ij}\frac{1}{N_j}\right] \tag{36}$$

where $f_{ti} = f_t(Sc, \overline{U}_i, I_u)$; $k_{ij} = 1$ for $j = \sqrt{2}\bar{\sigma}_{si}/\delta s + 1/2$, $\bar{\sigma}_{si}$ being the rms value of the self-excited stress for $\overline{U} = \overline{U}_i$; $k_{ij} = 0$ otherwise.

7. Applications

The proposed procedure is applied below to evaluate the crosswind induced fatigue of three steel chimneys, whose main characteristics are shown in Fig. 2, where R is the radius and t is the thickness of the shell. Chimney 1 (Fig. 2(a)) is 25 m high and has constant radius and thickness. Chimney 2 (Fig. 2(b)) is 100 m high and is composed by two trunks connected at $z = 34$ m; in order to decrease its tendency to lock-in, an inner layer of 5 cm of gunite is realised, which furnishes an added mass and increases the structural damping. Chimney 3 (Fig. 2(c)) is 30 m high and has constant radius and variable thickness. The steel of all the chimneys is Fe510. Table 1 summarizes the main dynamical properties of each structure.

Applying the Eurocode 1, the chimneys are placed in Italy, in zone 7, roughness class C, exposure category III. So, $k_T = 0.20$, $z_0 = 0.10$ m, $z_{\min} = 5$ m; furthermore, admitting that terrain is flat, $c_T = 1$. Thus, in correspondence with a mean return period of 50 years, $\overline{U}_{ref} = 29$ m/s (with $\Delta T = 10$ min).

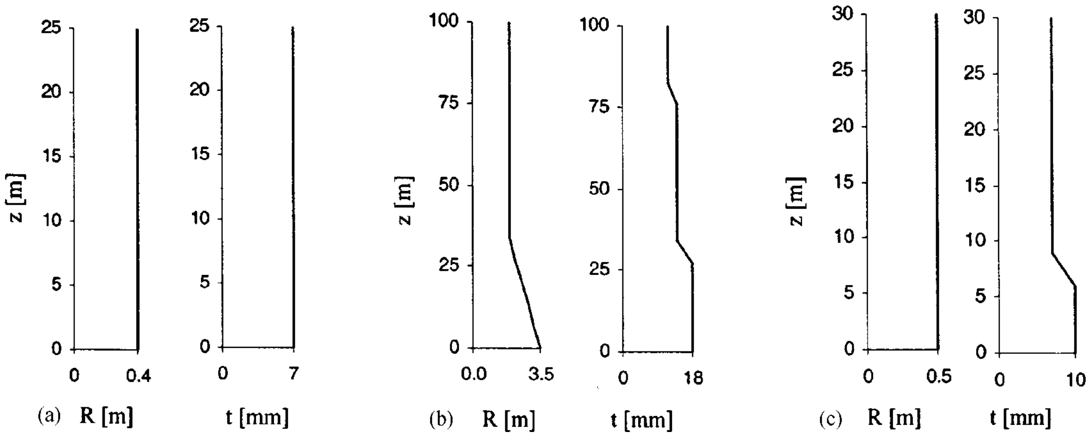

Fig. 2 Radius and thickness: (a) chimney 1; (b) chimney 2; (c) chimney 3

Table 1 Structural characteristics

Structure	Chimney 1	Chimney 2	Chimney 3
Height	$h = 25$ m	$h = 100$ m	$h = 30$ m
Fundamental frequency	$n_{y1} = 1.29$ Hz	$n_{y1} = 0.486$ Hz	$n_{y1} = 1.27$ Hz
Modal shape factor	$\zeta_{y1} = 1.5$	$\zeta_{y1} = 2$	$\zeta_{y1} = 1.7$
Structural damping	$\xi_{y1} = 0.006$	$\xi_{y1} = 0.01$	$\xi_{y1} = 0.006$
Scruton number	$Sc = 13.5$	$Sc = 16$	$Sc = 9.5$
Critical wind velocity	$\overline{U}_{cr}$=5 m/s	$\overline{U}_{cr} = 9$ m/s	$\overline{U}_{cr}$=6 m/s
Equivalent mass	$m_{y1} = 140$ kg/m	$m_{y1} = 2220$ kg/m	$m_{y1} = 160$ kg/m
Height of critical section	h_c=0 m	$h_c = 34$ m	$h_c = 0$ m

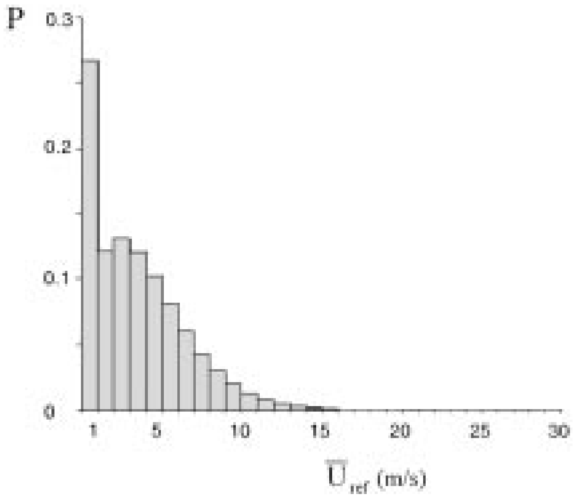

Fig. 3 Occurrence probability of the loading conditions

Taking this estimate into consideration, the dynamic response of all structures is determined for 30 loading conditions, assuming $\overline{U}_{ref,i} = (2i - 1)\delta\overline{U} / 2$, with $\delta\overline{U} = 1$ m/s, $i = 1, 2, \ldots, 30$. Analyses have been carried out to check the stability of the solution on decreasing $\delta\overline{U}$; they show that results do not change when using velocity intervals lower than 1 m/s. The occurrence probability of each loading condition is given by Eq. (27) using the parameters $F_0 = 0.1943$, $k = 1.549$, $c = 4.629$ m/s (Fig. 3).

Turbulence intensities at the site of the structures are $I_u(z) = 1/\ln(z / z_0)$, $I_v(z) = 0.8\ I_u(z)$; integral length scales are $L_u(z) = 300(z / 200)^{0.55}$, $L_v(z) = 0.25L_u(z)$ with z in metres; the exponential decay coefficient of the lateral turbulence is $C_{zv} = 6.5$ (Solari and Piccardo 2001). The drag coefficient of the shafts is $c_d = 0.7$, the rms lift wake coefficient is $\tilde{c}_{1\omega} = 0.3$, the Strouhal number is $S = 0.2$.

Fatigue damage is analysed in the critical structural sections reported in Table 1. According to the Eurocode 3 (1994), they are classified as Category 50 and the number of cycles N_j that causes the failure at different values of amplitude Δs_j is provided by the fatigue curve (Eq. 31) :

$$\begin{array}{lll} N_j \rightarrow \infty & \text{for} & \Delta s_j \leq \Delta s_L \\ N_j = a_1 / \Delta s_j^5 & \text{for} & \Delta s_L < \Delta s_j < \Delta s_D \\ N_j = a_2 / \Delta s_j^3 & \text{for} & \Delta s_D \leq \Delta s_j \end{array} \tag{37}$$

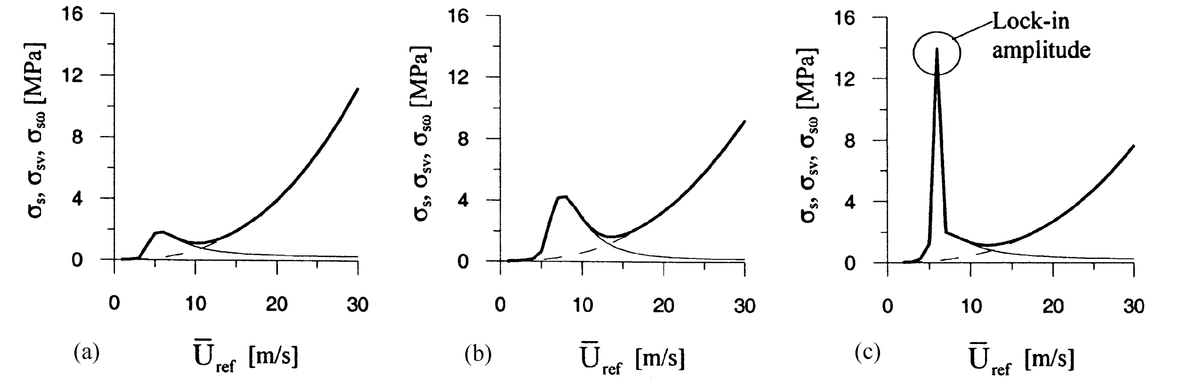

Fig. 4 Rms values of the stress processes in the critical sections: (a) chimney 1; (b) chimney 2; (c) chimney 3

where $a_1 = 3.436\times 10^{14}$, $a_2 = 2.518\times 10^{11}$, $\Delta s_L = 20$ MPa, $\Delta s_D = 37$ MPa. The parameters a_1 and a_2 take into account the partial safety factor $\gamma_{Mf} = 1.25$ advised by Eurocode 3 for fatigue resistance.

Fig. 4 shows the rms value of the fluctuating stress in the critical section of the three chimneys on varying the reference mean velocity $\overline{U}_{ref}$; thick lines correspond to the total stress; thin and dotted lines provide the contributions due to the lateral turbulence and to the vortex shedding, respectively. Diagram a) is referred to chimney 1 and shows that vortex shedding effects in the low wind velocity range are quite limited, while lateral turbulence effects dominate at high wind velocity values. Diagram b) is referred to chimney 2 where vortex shedding effects on the response are more evident, although lateral turbulence effects still dominate at high wind velocity values. Diagram c) is referred to chimney 3 where the crosswind response is characterised by a lock-in phenomenon in correspondence of the critical wind velocity. In particular, using ESDU method, $f_t = 0.66$ for $\overline{U} = \overline{U}_{cr}$, $f_t = 0$ for $\overline{U} \neq \overline{U}_{cr}$. Due to such phenomenon, vortex shedding effects in the low wind velocity range is larger than lateral turbulence effects at high wind velocity values.

As the yielding limit stress of the structural material is $f_y = 235$ Mpa, the three structures exhibite, due to crosswind vibrations, a consistent safety margin as regard the ultimate limit state. Other analyses not reported here showed that the ultimate limit state verification is satisfied also taking the alongwind response into account.

Fig. 5 illustrates the 3D stress cycles histogram (Eq. 36) induced by crosswind vibrations in the critical sections of the three chimneys during 1 year. These diagrams show numerous blocks at low wind velocity due to vortex shedding and some smaller blocks at high wind velocity due to lateral turbulence. The most relevant differences occur in the range of the critical velocities. Fig. 5(a) shows few and small blocks. Fig. 5(b) points out the presence of some blocks characterised by large amplitude. Fig. 5(c) emphasises one dominant block associated with high stress amplitude.

Applying Eq. (30) in correspondence of Eq. (37), the fraction of the damage induced to structures by any block of the cycle histogram is shown in Fig. 6 on varying the amplitude of the stress cycles and the reference velocity. It is worth notice that diagrams (a), (b) and (c) adopt different vertical scales.

Fig. 6(a) shows the distribution of the damage induced in chimney 1. It is concentrated in two ranges of the wind velocity, where the greatest amplitude cycles arise due to vortex shedding and lateral turbulence, respectively. In this case vortex shedding and lateral turbulence contributions to fatigue damage are of the same order of magnitude. However, this chimney does not suffer wind induced fatigue, as the mean fatigue life is $T_F = 2\times 10^3$ years (Eq. 32).

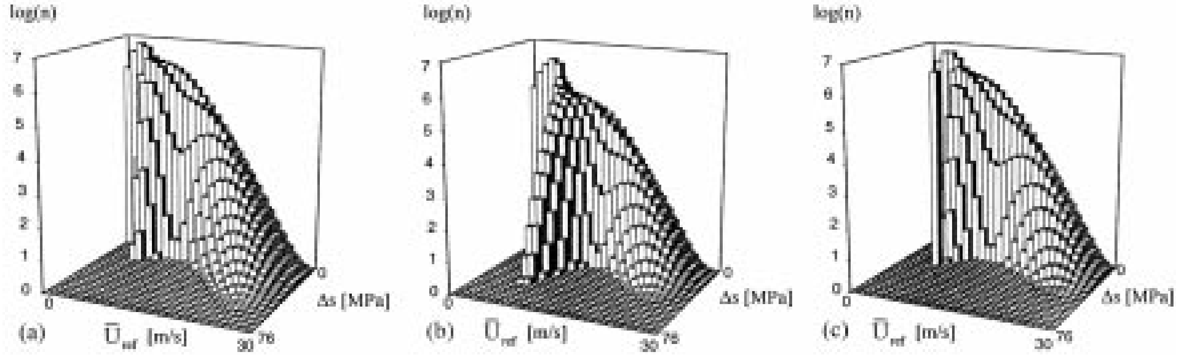

Fig. 5 Histogram of the stress cycles: (a) chimney 1; (b) chimney 2; (c) chimney 3

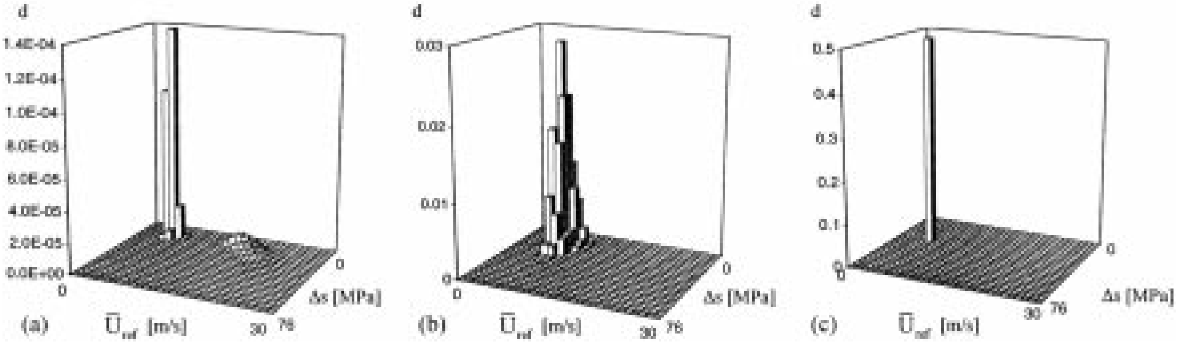

Fig. 6 Fractions of damage: (a) chimney 1; (b) chimney 2; (c) chimney 3

The fraction of the damage induced in chimney 2 is represented in Fig. 6(b). The damage is concentrated in the intermediate range of the wind velocity, where great amplitude cycles due to vortex shedding arise. The blocks at higher wind velocity, due to lateral turbulence, cause negligible damage. The corresponding mean fatigue life is $T_F = 47$ years (Eq. 32). The fatigue phenomenon is dominated by the vortex shedding, contrary to the limit state verification, which pointed out the dominant role of the gust buffeting.

Fig. 6(c) shows the distribution of the damage in chimney 3. It is caused by only the block of the cycles induced in correspondence of the critical velocity responsible of the lock-in phenomenon; other contributions to damage are negligible. The corresponding mean fatigue life is $T_F = 1.8$ years (Eq. 36). This means that the structure, judged as safe with regard to ultimate limit states, is absolutely unsafe due to fatigue.

The obtained solutions are compared with the results of a numeric analysis carried out by Monte Carlo simulations. Chimney 2 is taken into account and 30 stress histories at the critical section, associated with 30 loading conditions, were carried out by the random phase method (Shinozuka and Jan 1972), starting from the stress spectrum in Eq. (12). Each stress time history was simulated over a period of $\Delta T = 10$ minutes, with a time step $\Delta t = 0.1$s. Fig. 7 shows some pieces of the simulated stress histories, corresponding to different values of the reference wind velocity; the diagrams confirm that the narrow band hypothesis may be correctly applied to crosswind stress processes, especially in the range of the critical wind velocity.

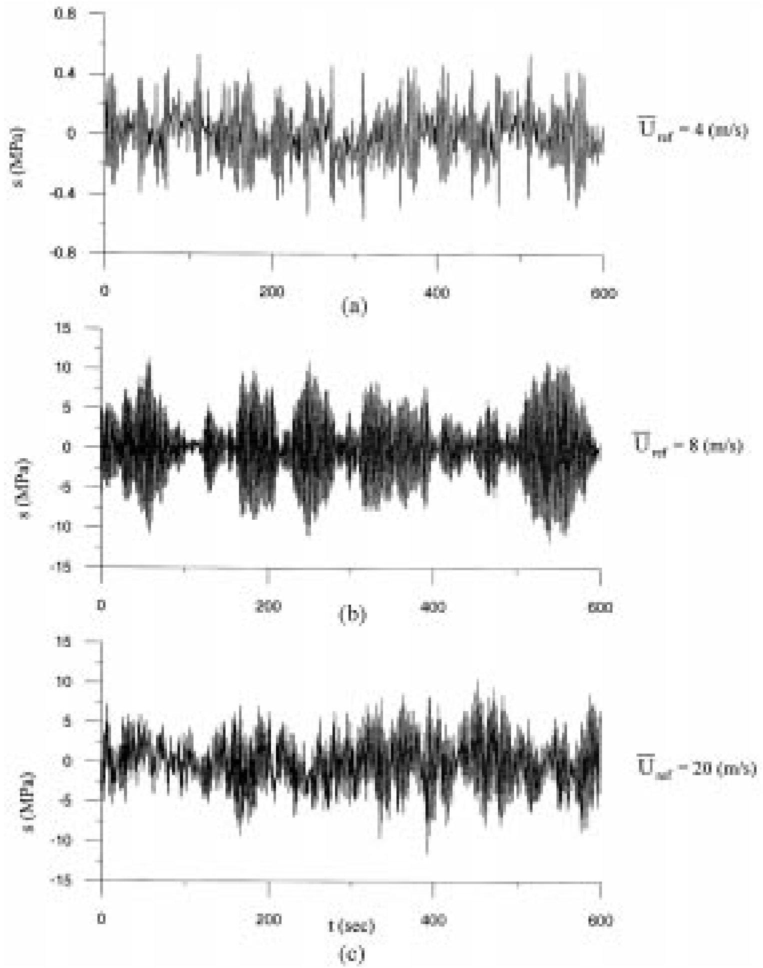

Fig. 7 Simulated stress histories in chimney 2: (a) $\overline{U}_{ref}$ = 4 m/s; (b) $\overline{U}_{ref}$ = 8 m/s; (c) $\overline{U}_{ref}$ = 20 m/s

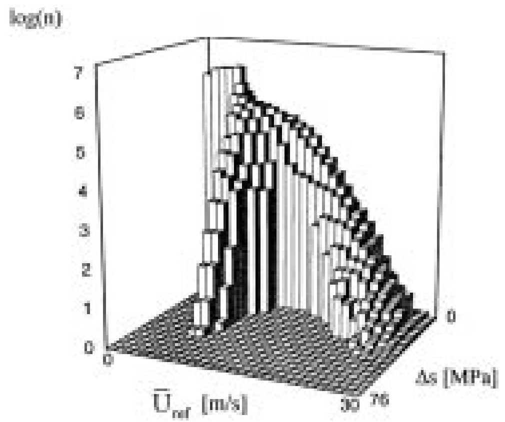

Fig. 8 Histogram of the stress cycles obtained by the rainflow method (chimney 2)

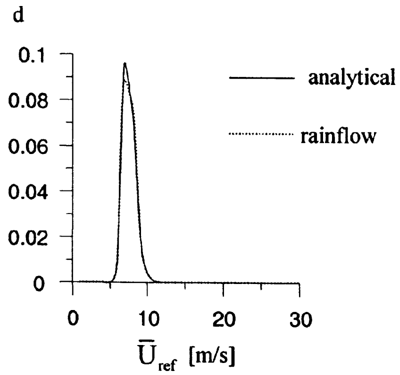

Fig. 9 Fractions of damage caused by each loading condition (chimney 2)

Each history has been analysed by means of a cycle counting algorithm based on the rainflow method (Rychlik 1987); the number of cycles during 10 minutes was extended to the reference period $T = 1$ year by taking into account the occurrence probability of each loading condition (Fig. 2). Fig. 8 shows the stress cycle histogram given by the above procedure and confirms that the results are in good agreement with those obtained applying Eq. (28) (Fig. 5b). Fig. 9 shows the fractions of the damage associated to each loading conditions, evaluated with the proposed analytical method and with the rainflow method. The rainflow results endorse the analytical estimate both in the damage distribution and in the fatigue life ($T_F = 48$ years), attesting the precision of the proposed method for crosswind vibrations where the narrow band hypothesis is satisfied.

8. Conclusions

This paper proposes a mathematical method for fatigue analysis of slender vertical structures subjected to crosswind vibrations. Lateral turbulence and vortex shedding actions on stationary structures are schematised by spectral models. Lock-in effects are taken into account though ESDU method. Expressions of the cycles histogram and of the mean fatigue life are determined in a probabilistic environment. They highlight the great importance of the vortex shedding mechanism in the damage accumulation, even if the ultimate limit state verifications are widely satisfied. The comparison between theoretical and numerical solutions, obtained processing Monte Carlo simulations by the rainflow technique, confirms the precision of the proposed method.

A research is currently in progress with the aim of improving the analysis by taking into account the contribution of all vibration modes to the static and quasi-static parts of the stress (Piccardo and Solari 2002, Solari and Repetto 2001), by considering the damage reduction due to the dominant role of directional wind velocity distributions and by superimposing the alongwind and crosswind stresses to evaluate the global accumulated damage (Repetto and Solari 2001b).

References

Basis of Design and Actions on Structures, Eurocode 1, Part 2-4:Wind Actions, ENV 1991-2-4, European Committee for Standardisation, Brussels (1994).

Davenport, A.G. (1966), "The estimation of load repetitions on structures with application to wind induced fatigue and overload", *RILEM International Symposium on the Effects of Repeated Loading of Materials and Structures*, Mexico City, September, 1-18.

Design of Steel Structures, Part 1-1: General Rules and Rules for Buildings, ENV 1993, European Committee for standardisation, Brussels (1994).

Mikitarenko, M.A. and Perelmuter, A.V. (1997), "Safe fatigue life of steel towers under the action of wind vibrations", *J. Wind Eng. Ind. Aerod.*, **74-76**, 1091-1100.

Peil, U. and Behrens, M. (2002), "Fatigue of tubular steel lighting colums under wind load", *Wind and Struct.*, **5**, 463-478.

Petrov, A.A. (1998), "Dynamic response and life prediction of the steel structures under wind loading", *J. Wind Eng. Ind. Aerod.*, **74-76**, 1057-1065.

Piccardo, G. and Solari, G. (1998), "Generalized equivalent spectrum technique", *Wind and Struct.*, **1**, 161-174.

Piccardo, G. and Solari, G. (2000), "3-D wind-excited response of slender structures: closed form solution", *J. Struct. Eng., ASCE*, **126**, 936-943.

Piccardo, G. and Solari, G. (2002), "3-D gust effects factor for slender vertical structures", *Prob. Eng. Mech.*, **17,** 143-155.

Repetto, M.P. and Solari, G. (2001a), "Dynamic alongwind fatigue of slender vertical structures", *Eng. Struct.*, **23**, 1622-1633.

Repetto, M.P. and Solari, G. (2001b), "An advanced model for estimating the wind-induced fatigue of slender structures", *Proc. of 3rd European & African Conference on Wind Engineering*, Eindhoven, July, 263-270.
Response of structures to vortex shedding. Structures of circular or polygonal cross section. Item 96030, ESDU International, London (1996).
Robertson, A.P., Hoxey, R.P., Short, J.L. and Burges L.R. (1999), "Wind-induced fatigue loading of tubular steel lighting columns", *Proc of the 10th Int. Conf on Wind Engng, Copenhagen*, Denmark, June, 537-544.
Ruscheweyh, H. (1994), "Vortex excited vibrations", in *Wind-Excited Vibrations of Structures*, Sockel H. ed., Springer-Verlag, Wien, 51-84.
Rychlik, I. (1987), "A new definition of the rainflow cycle counting method", *Int. J Fatigue*, **9**, 119-121.
Shinozuka, M. and Jan, C.M. (1972), "Digital simulation of random processes and its applications", *J. Sound Vib.*, **25**, 111-128.
Solari, G. (1985), "Mathematical model to predict 3-D wind loading on buildings", *J. Eng. Mech.*, ASCE, **111,** 254-276.
Solari, G. (1986), "3-D response of buildings to wind action", *J. Wind Eng. Ind. Aerod.*, **21**, 379-393.
Solari, G. (1996), "Wind speed statistics", in *Modelling of Atmospheric Flow Fields.* Lalas and Ratto ed., World Scientific Publishing, Singapore, 637-657.
Solari, G. (1999), "Progress and prospects in gust-excited vibrations of structures", *Eng. Mech.*, **6**, 301-322.
Solari, G. and Piccardo, G. (2001), "Probabilistic 3-D turbulence modeling for gust-buffeting of structures", *Prob. Eng. Mech.*, **16**, 73-86.
Solari, G. and Repetto, M.P. (2001), "3-D gust-excited effects on vertical structures", *Proc. of 3rd European & African Conference on Wind Engineering*, Eindhoven, July, 255-262.
Van de Hoven, I. (1957), "Power spectrum of wind velocity fluctuations in the frequency range from 0.0007 to 900 cycles per hour", *J. Meteor.*, **14**, 1254-1255.
Vickery, B.J. and Basu, R.I. (1983), "Across-wind vibrations of structures of circular cross-section. Part I: development of a mathematical model for two-dimensional conditions", *J. Wind Eng. Ind. Aerod.*, **12**, 49-74.
Vickery, B.J. and Clark, A.W. (1972), "Lift or across-wind response of tapered stacks", *J. Struct. Div.*, ASCE, **98**, 1-20.

Appendix - I

Adopting the turbulence model proposed by Solari and Piccardo (2001), the spectral equation of the reduced turbulence component v^* is given by :

$$S_v^*(z, n) = \frac{9.434\dfrac{L_v(z)}{\bar{U}(z)}}{\left(1 + 14.151\dfrac{nL_v(z)}{\bar{U}(z)}\right)^{5/3}} \tag{38}$$

where $\bar{U}$ is the mean wind velocity and L_v is the integral length scale of v in y direction. The coherence function of v is expressed by the relationship:

$$\mathrm{Coh}_{vv}(z, z', n) = \exp\left\{-\frac{2nC_{zv}|z - z'|}{\bar{U}(z) + \bar{U}(z')}\right\} \tag{39}$$

where C_{vz} is the exponential decay coefficient of v along z.

The spectral equation of the reduced wake excitation in y direction is expressed by the model proposed by Vickery and Clark (1972):

$$S_\omega^*(z, n) = \frac{1}{\sqrt{\pi}B(z)n_\omega(z)}\exp\left\{-\left[\frac{1 - n/n_\omega(z)}{B(z)}\right]^2\right\} \tag{40}$$

where $n_\omega(z) = S\overline{U}(z) / b$ is the vortex shedding frequency, S is the Strouhal number, b is the width of the section; $B(z)$ is the bandwidth spectral parameter assigned by the formula $B^2(z) = B_0^2 + 2I_u^2(z)$, where I_u is the longitudinal turbulence intensity and $B_0 = 0.08$. The wake coherence function is given by ESDU (*Response of Structures* 1996):

$$\mathrm{Coh}_{\omega\omega}(z, z', n) = \exp\left\{-\frac{|z - z'|}{Lb}\right\} \tag{41}$$

where L is the correlation length (in b's) of the vortex shedding.

Appendix - II

Considering the spectral equations given in Appendix I, the quasi-static and the resonant terms in Eq. (25) assume the form (Piccardo and Solari 2000):

$$Q_v = \frac{1}{1 + 0.25\left(\dfrac{k_{yv}C_{zv}h}{L_v(z_{yv})}\right)^{0.63}} \tag{42}$$

$$D_v = \frac{\pi}{4\xi_{y1}} \frac{9.434\left[\dfrac{n_{y1}L_v(z_{yv})}{\overline{U}(z_{yv})}\right]}{\left\{1 + 14.151\left[\dfrac{n_{y1}L_v(z_{yv})}{\overline{U}(z_{yv})}\right]\right\}^{5/3}} C\left\{k_{yv}\frac{n_{y1}C_{zv}h}{\overline{U}(z_{yv})}\right\} \tag{43}$$

$$Q_\omega = C\left\{\frac{k_{y\omega}h}{Lb}\right\}F\left\{\frac{n_{y1}}{n_\omega(z_{y\omega})}\right\} \tag{44}$$

$$D_\omega = \frac{\pi}{4\xi_{y1}} \frac{n_{y1}/n_\omega(z_{y\omega})}{\sqrt{\pi}B(z_{y\omega})} \exp\left\{-\left[\frac{1 - \{n_{y1}/n_\omega(z_{y\omega})\}}{B(z_{y\omega})}\right]^2\right\} C\left\{\frac{k_{y\omega}h}{Lb}\right\} \tag{45}$$

where F is a function defined as:

$$F\{\omega\} = \frac{\omega^4}{\omega^4 - 3\omega^2 + 4} \tag{46}$$

In the above equations, b and h are the reference size of the cross-section and the height of the structure, respectively. $\overline{U}$ is the mean wind velocity, L_v is the integral length scale of v in y direction and C_{zv} is the exponential decay coefficient of v along z. n_{y1} and ξ_{y1} are the fundamental frequency and the damping coefficient of the first mode in y direction, respectively. $z_{yv} = 0.6$ h and $z_{y\omega} = 0.8$ h are the reference co-ordinates; $k_{yv} = k_{y\omega} \simeq 0.5 / (\zeta_{y1} + 1)^{0.55}$ are the equivalent correlation factors, where ζ_{y1} is a modal shape factor. $n_\omega(z) = S\overline{U}(z) / b$ is the vortex shedding frequency, S is the Strouhal number, $B(z)$ is the bandwidth spectral parameter. L is the correlation length, expressed in b's. C is defined by Eq. (22).

CC